

## **QUARK–GLUON PLASMA, COLOR GLASS CONDENSATE AND GLASMA: 3 LECTURES AT LAKE BAIKAL**

*L. McLerran*<sup>1</sup>

Brookhaven National Laboratory and RIKEN Brookhaven Center, Physics Dept., Upton, NY, USA

These lectures concern the properties of strongly interacting matter at very high energy density. I begin with the properties of the Quark–Gluon Plasma and Quarkyonic Matter. I later discuss the Color Glass Condensate and the Glasma, matter that controls the earliest times in hadronic collisions. I then describe the Quark–Gluon Plasma, matter produced from the thermalized remnants of the Glasma. The discussion will be intuitive and based on simple structural aspects of QCD. There will be some discussion of experimental tests of these ideas.

Предлагаются лекции о свойствах сильно взаимодействующего вещества при очень высоких плотностях энергии. Вначале обсуждаются свойства кварк-глюонной плазмы и кварковой материи. Затем рассматриваются конденсат цветного стекла и глазма — вещества, контролирующие самые ранние времена в адронных столкновениях. Далее описывается кварк-глюонная плазма — вещество, наработанное из термализованных остатков глазмы. Обсуждение проводится на интуитивном уровне и основано на простых структурных аспектах КХД. Также обсуждаются некоторые экспериментальные проверки этих идей.

PACS: 12.38.Mh; 25.75.Nq

### **INTRODUCTION**

These lectures concern the properties of strongly interacting matter at high energy density. Such matter occurs in a number of contexts. The high-density partonic matter that controls the early stages of hadronic collisions at very high energies is largely made of very coherent gluonic fields. In a single hadron, such matter forms the small  $x$  part of a wavefunction, a Color Glass Condensate. After a collision of two hadrons, this matter almost instantaneously is transformed into longitudinal color electric and color magnetic fields. The ensemble of these fields in their early time evolution is called the Glasma. The decay products of these fields thermalize and form a high-temperature gas of quarks and gluons, the Quark–Gluon Plasma. In collisions at lower energy, and perhaps in naturally occurring objects such as neutron stars, there is high baryon density matter at low temperature. This is Quarkyonic matter.

---

<sup>1</sup>E-mail: mclerran@mac.com

There is a very well developed literature concerning these various forms of matter. It is not the purpose of these lectures to provide a comprehensive review. I will concentrate on motivating and describing such matter from simple intuitive physical pictures and from simple structural aspects of QCD. I will attempt at various places to relate what is conjectured or understood about such matter to experimental results from accelerator experiments.

## 1. LECTURE I: MATTER AT HIGH TEMPERATURE: THE QUARK–GLUON PLASMA

**1.1. Matter at Finite Temperature.** In this lecture I will describe the properties of matter at high temperature. The discussion here will be theoretical. There is a wide literature on the phenomenology of the Quark–Gluon Plasma and its possible description of heavy-ion collisions at RHIC energies. The interested reader is referred to that literature. I will here develop the ideas of deconfinement, chiral symmetry restoration based in part on a simple description using the large number of colors limit of QCD.

**1.2. Confinement.** The partition function is

$$Z = \text{Tr} e^{-\beta H + \beta \mu_B N_B}, \quad (1)$$

where the temperature is  $T = 1/\beta$ ,  $N_B$  is the baryon number and  $\mu_B$  is the baryon number chemical potential. Operator expectation values are

$$\langle O \rangle = \frac{\text{Tr} O e^{-\beta H + \beta \mu_B N_B}}{Z}. \quad (2)$$

Under the substitution  $e^{-\beta H} \rightarrow e^{-itH}$ , the partition function becomes the time evolution operator of QCD. Therefore, if we change  $t \rightarrow it$ , redefine zeroth components of fields by appropriate factors of  $i$ , and introduce Euclidean gamma matrices with anticommutation relations

$$\{\gamma^\mu, \gamma^\nu\} = -2\delta^{\mu\nu}, \quad (3)$$

then for QCD, the partition function has the path integral representation

$$Z = \int [dA][d\bar{\psi}][d\psi] \exp \left\{ - \int_0^\beta d^4x \left( \frac{1}{4} F^2 + \bar{\psi} \left[ \frac{1}{i} \gamma D + m + i\mu_Q \gamma^0 \right] \psi \right) \right\}. \quad (4)$$

Here the fermion field is a quark field so that the baryon number chemical potential is

$$\mu_Q = \frac{1}{N_c} \mu_B. \quad (5)$$

This path integral is in Euclidean space and is computable using Monte Carlo methods when the quark chemical potential vanishes. If the quark chemical potential is nonzero, various contributions appear with different sign, and the Monte Carlo integrations are poorly convergent. Boundary conditions on the fields must be specified on account of the finite length of the integration in time. They are periodic for Bosons and antiperiodic for Fermions, and follow from the trace in the definition of the partition function.

A straightforward way to probe the confining properties of the QCD matter is to introduce a heavy test quark. If the free energy of the heavy test quark is infinite, then there is confinement, and if it is finite there is deconfinement. We shall see below that the free energy of a quark added to the system is

$$e^{-\beta F_q} = \langle L \rangle, \tag{6}$$

where

$$L(\mathbf{x}) = \frac{1}{N_c} \text{Tr} P \exp \left[ i \int dt A^0(\mathbf{x}, t) \right]. \tag{7}$$

So confinement means  $\langle L \rangle = 0$  and deconfinement means that  $\langle L \rangle$  is finite. The path ordered phase integration which defines the line operator  $L$  is shown in Fig. 1. Such a path ordered phase is called a Polyakov loop or Wilson line.

It is possible to prove that the free energy of a heavy static quark added to the system is given by Eq. (6) using the effective action for a very heavy quark:

$$S_{\text{HQ}} = \int dt \bar{\psi}(\mathbf{x}, t) \frac{1}{i} \gamma^0 D^0 \psi(\mathbf{x}, t). \tag{8}$$

The Yang–Mills action is invariant under gauge transformations that are periodic up to an element of the center of the gauge group. The center of the gauge group is a set of diagonal matrices  $Z_p = e^{2\pi i p/N} \bar{I}$ , where  $\bar{I}$  is an identity matrix.



Fig. 1. The contour in the  $t$  plane which defines the Polyakov loop. The space is closed in time because of the periodic boundary conditions imposed by the definition of the partition function

The quark contribution to the action is not invariant, and  $L \rightarrow Z_p L$  under this transformation. In a theory with only dynamical gluons, the energy of a system of  $n$  quarks minus antiquarks is invariant under the center symmetry transformation only if  $n$  is an integer multiple of  $N$ . Therefore, when the center symmetry is realized, the only states of finite free energy are baryons plus color singlet mesons.

The realization of the center symmetry,  $L \rightarrow Z_p L$ , is equivalent to confinement. This symmetry is like the global rotational symmetry of a spin system, and it may be either realized or broken. At large separations, the correlation of a line and its adjoint, corresponding to a quark–antiquark pair, is

$$\lim_{r \rightarrow \infty} \langle L(r) L^\dagger(0) \rangle = C e^{-\kappa r} + \langle L(0) \rangle \langle L^\dagger(0) \rangle, \tag{9}$$

since upon subtracting a mean field term, correlation functions should vanish exponentially. Since

$$e^{-\beta F_{q\bar{q}}(r)} = \langle L(r) L^\dagger(0) \rangle, \tag{10}$$

we see that in the confined phase, where  $\langle L \rangle = 0$ , the potential is linear, but in the unconfined phase, where  $\langle L \rangle$  is nonzero, the potential goes to a constant at large separations.

The analogy with a spin system is useful. For the spin system corresponding to QCD without dynamical quarks, the partition function can be written as

$$Z = \int [dA] \exp \left( -\frac{1}{g^2} S[A] \right). \tag{11}$$

The effective temperature of the spin system associated with the gluon fields is  $T_{\text{eff}} \sim g^2$ . By asymptotic freedom of the strong interactions, as real temperature gets larger, the effective temperature gets smaller. So at large real temperature (small effective temperature) we expect an ordered system, where the  $Z_N$  symmetry is broken, and there is deconfinement. For small real temperature corresponding to large effective temperature, there is disorder or confinement.

The presence of dynamical fermions breaks the  $Z_N$  symmetry. This is analogous to placing a spin system in an external magnetic field. There is no longer any symmetry associated with confinement, and the phase transition can disappear. This is what is believed to happen in QCD for physical masses of quarks. What was a first-order phase transition for the theory in the absence of quarks becomes a continuous change in the properties of the matter for the theory with quarks.

Another way to think about the confinement–deconfinement transition is a change in the number of degrees of freedom. At low temperatures, there are light meson degrees of freedom. Since these are confined, the number of degrees of freedom is of order one in the number of colors. In the unconfined world, there are  $2(N_c^2 - 1)$  gluons and  $4N_c N_f$  fermions, where  $N_f$  is the number of light-mass fermion families. The energy density scaled by  $T^4$  is a dimensionless number and directly proportional to the number of degrees of freedom. We expect it to have the property shown in Fig. 2 for pure QCD in the absence of quarks. The discontinuity at the deconfinement temperature,  $T_d$ , is the latent heat of the phase transition.

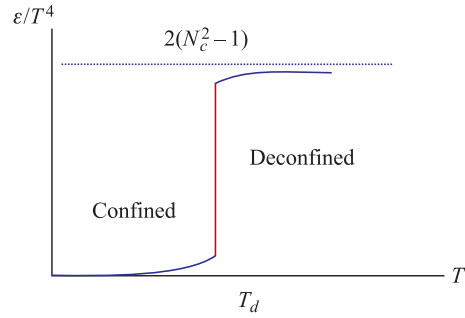


Fig. 2. The energy density scaled by  $T^4$  for QCD in the absence of dynamical quarks

The energy density can be computed using lattice Monte Carlo methods. The result of such computation is shown in Fig. 3. The discontinuity present for the theory with no quarks becomes a rapid crossover when dynamical quarks are present.

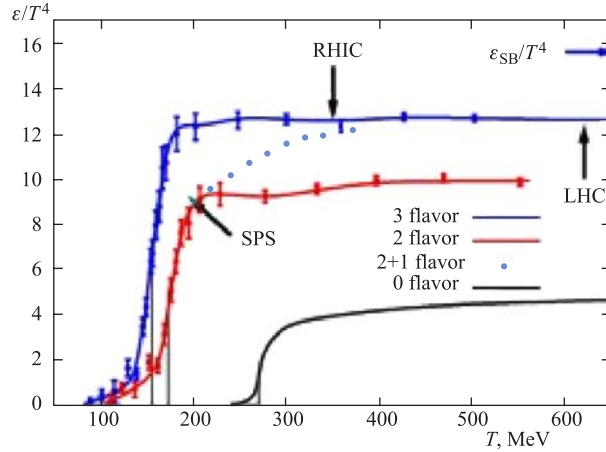


Fig. 3. The energy density scaled by  $T^4$  measured in QCD from lattice Monte Carlo simulation. Here there are quarks with realistic masses

The large  $N_c$  limit gives some insight into the properties of high-temperature matter [1–4]. As  $N_c \rightarrow \infty$ , the energy density itself is an order parameter for the deconfinement phase transition. Viewed from the hadronic world, there is an amount of energy density  $\sim N_c^2$  which must be inserted to surpass the transition temperature. At infinite  $N_c$  this cannot happen, as this involves an infinite amount of energy. There is a Hagedorn limiting temperature, which for finite  $N_c$  would have been the deconfinement temperature.

The Hagedorn limiting temperature can be understood from the viewpoint of the hadronic world as arising from an exponentially growing density of states. In a few paragraphs, we will argue that mesons and glueballs are very weakly interacting in the limit of large  $N_c$ . Therefore, the partition function is

$$Z = \int dm \rho(m) e^{-m/T}. \tag{12}$$

Taking  $\rho(m) \sim m^\alpha e^{\kappa m}$ , so that

$$\langle m \rangle \sim \frac{1}{1/T - \kappa} \tag{13}$$

diverges when  $T \rightarrow 1/\kappa$ .

**1.3. A Brief Review of the Large  $N_c$  Limit.** The large  $N_c$  limit for an interacting theory takes  $N_c \rightarrow \infty$  with the 't Hooft coupling  $g_{t\text{Hooft}}^2 = g^2 N_c$  finite. This approximation has the advantage that the interactions among quarks and gluons simplify. For example, at finite temperature, the disappearance of confinement is associated with Debye screening by gluon loops, as shown in Fig. 4, *a*. This diagram generates a screening mass of order  $M_{\text{screen}}^2 \sim g_{t\text{Hooft}}^2 T^2$ . On the other hand, the quark loop contribution is smaller by a power of  $N_c$  and vanishes in the large  $N_c$  limit.

To understand interactions, consider Fig. 5, *a*. This corresponds to a mesonic current–current interaction through quarks. In powers of  $N_c$ , it is of order  $N_c$ . Gluon interactions will not change this overall factor. The three-current interaction is also of order  $N_c$ , as shown in Fig. 5, *b*. The three-meson vertex  $G$ , which remains after amputating the external lines, is therefore of order  $1/\sqrt{N_c}$ . A similar argument shows that the four-meson interaction is of order  $1/N_c$ . Using the same arguments, one can show that the 3-gluon vertex is of order  $1/N_c$  and the four-gluon interaction of order  $1/N_c^2$ .

These arguments show that QCD at large  $N_c$  becomes a theory of noninteracting mesons and glueballs. There are an infinite number of such states because excitations can never decay. In fact, the spectrum of mesons seen in nature does look to a fair approximation like noninteracting particles. Widths of resonances are typically of order 200 MeV, for resonances with masses up to several GeV.

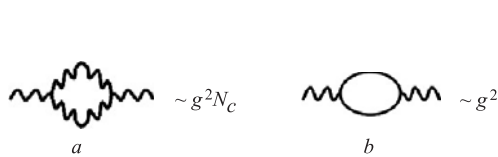


Fig. 4. *a*) The gluon loop contribution to the heavy-quark potential. *b*) The quark loop contribution to the potential

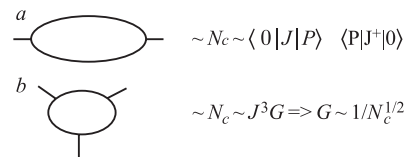


Fig. 5. *a*) The quark loop corresponding to a current–current interaction. *b*) A quark loop corresponding to a three-current interaction

**1.4. Mass Generation and Chiral Symmetry Breaking.** QCD in the limit of zero quark masses has a  $U(1) \times SU_L(2) \times SU_R(2)$  symmetry. (The  $U_5(1)$  symmetry is explicitly broken due to the axial anomaly.) Since the pion field  $\bar{\psi}\tau^a\gamma_5\psi$  is generated by an  $SU_{L-R}(2)$  transformation of the sigma field  $\bar{\psi}\psi$ , the energy (or potential) in the space of the pion-sigma field is degenerate under this transformation. In nature, pions have anomalously low masses. This is believed to be a consequence of chiral symmetry breaking, where the  $\sigma$  field acquires an expectation value, and the pion fields are Goldstone bosons associated with the degeneracy of the potential under the chiral rotations.

Such symmetry breaking can occur if the energy of a particle–antiparticle pair is less than zero, as shown in Fig. 6. On the left of this figure is the naive vacuum where the negative energy states associated with quark are filled. The right-hand side of the figure corresponds to a particle hole excitation, corresponding to a sigma meson. Remember that a hole in the negative energy sea corresponds to an antiparticle with the opposite momentum and energy. If the  $\sigma$ -meson excitation has negative energy, the system is unstable with respect to forming a condensate of these mesons.

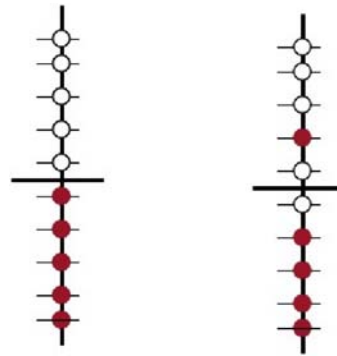


Fig. 6. The energy levels of the Dirac equation. Unfilled states are open circles and filled states are solid circles. For the free Dirac equation, negative energy states are filled and positive energy states are unoccupied, as shown on the left-hand side. A mesonic excitation corresponding to a particle–hole pair is shown on the right-hand side

At sufficiently high temperature, the chiral condensate might melt. Indeed this occurs [5]. For QCD, the chiral and deconfinement phase transitions occur at the same temperature. At a temperature of about 170–200 MeV, both the linear potential disappears and chiral symmetry is restored. It is difficult to make a precise statement about the identification of the chiral and deconfinement phase transitions, since as argued above, for QCD with quarks, there is not a real phase transition associated with deconfinement [6,7]. Also, when quarks have finite masses, as they do in nature, chiral symmetry is not an exact symmetry, and there need be no strict phase transition associated with its restoration. Nevertheless, the crossover is quite rapid, and there are rapid changes in both the potential and the sigma condensate  $\langle\bar{\psi}\psi\rangle$  at temperatures which are in a narrow range.

## 2. LECTURE II: MATTER AT HIGH BARYON NUMBER DENSITY: QUARKYONIC MATTER

I now turn to a discussion of the phase diagram of QCD at finite baryon number density.

In the large  $N_c$  limit of QCD, the nucleon mass is of order  $N_c$  [1–3]. This means that in the confined phase of hadronic matter, for baryon chemical potential  $\mu_B \leq M_N$ , the baryon

number density is essentially zero:

$$\langle N_B \rangle \sim e^{(\mu_B - M_N)/T} \sim e^{-N_c}. \quad (14)$$

For temperatures above the deconfinement phase transition, the baryon number is nonzero since there the baryon number density is controlled by  $e^{-M_q/T} \sim 1$ , and quark masses are independent of  $N_c$ . For sufficiently large chemical potential, the baryon number density can be also nonzero. The Hadronic Matter phase of QCD is characterized in large  $N_c$  by zero baryon number density, but at higher density there is a new phase.

In the large  $N_c$  limit, fermion loops are suppressed by a factor of  $1/N_c$ . Therefore, the contribution to Debye screening from quarks cannot affect the quark potential until

$$M_{\text{Debye}}^2 \sim \alpha_{\text{tHooft}} \mu_{\text{quark}}^2 / N_c \sim \Lambda_{\text{QCD}}^2. \quad (15)$$

Here the quark chemical potential is  $\mu_B = N_c \mu_{\text{quark}}$ . The relationship involving the Debye mass means there is a region parametrically large chemical potential  $M_N \leq \mu_B \leq \sqrt{N_c} M_N$  where matter is confined, and has finite baryon number. This matter is other than either the Hadronic Matter or the Deconfined Phases. It is called Quarkyonic because it exists at densities parametrically large compared to the QCD scale, where quark degrees of freedom are important, but it is also confined so the degrees of freedom may be thought of also as those of confined baryons [8,9].

The width of the transition region between the Hadronic phase and the Quarkyonic phase is estimated by requiring that the baryon number density become of order  $N_B/V \sim k_{\text{Fermi}}^3 \sim \Lambda_{\text{QCD}}^3$ . Recall that the baryon chemical potential is  $\mu_B \sim M_N + k_f^2/2M_N$  for small  $k_f$ , so that the width of the transition in  $\mu_B$  is very narrow, of order  $1/N_c$ . This is  $\delta\mu_{\text{quark}} \sim 1/N_c^2$  when expressed in terms of  $\mu_{\text{quark}}$  which is the finite variable in the large  $N_c$  limit.

The transition from Hadronic Matter to that of the Quark–Gluon Plasma may be thought of as a change in the number of degrees of freedom of matter. Hadronic Matter at low temperatures has 3 pion degrees of freedom. The quark–gluon plasma has of order  $2(N_c^2 - 1)$  degrees of freedom corresponding to gluons and  $4N_c$  degrees of freedom for each light-mass quark. The change in degrees of freedom is of order  $N_c^2$  in the large  $N_c$  limit. At very high baryon number densities, the quarks in the Fermi sea interact at short distances, and although strictly speaking are confined, behave like free quarks. The number of degrees of freedom is therefore of order  $N_c$ . Each phase has different numbers of degrees of freedom, and is presumably separated from the other by a rapid crossover.

Quarkyonic matter is confined and therefore thermal excitations such as mesons, glueballs, and Fermi surface excitations must be thought of as confined. The quarks in the Fermi sea are effectively weakly interacting since their interactions take place at short distances. So in some sense, the matter is «deconfined» quarks in the Fermi sea with confined glueball, mesons and Fermi surface excitations [10].

In Hadronic Matter, chiral symmetry is broken and in Deconfined Matter it is broken. In Quarkyonic Matter chiral symmetry is broken by the formation of charge density waves from binding of quark and quark hole excitations near the Fermi surface [11]. In order that the quark hole have small relative momentum to the quark, the quark hole must have momentum opposite to that of the quark. This means the quark–quark hole excitation has total net momentum, and therefore the finite wavelength of the corresponding bound state leads to a breaking of translational invariance. The chiral condensate turns out to be a chiral

spiral where the chiral condensate rotates between different Goldstone bosons as one moves through the condensate [12]. Such condensation may lead to novel crystalline structures [13].

A figure of the hypothetical phase diagram of QCD is shown in Fig. 7 for  $N_c = 3$ . Also shown is the weak liquid–gas phase transition, and the phase associated with color superconductivity. Although the color superconducting phase cannot coexist with quarkyonic matter in infinite  $N_c$ , for finite  $N_c$  there is such a possibility. The lines on this phase diagram might correspond to true phase transitions or rapid crossovers. The confinement–deconfinement tran-

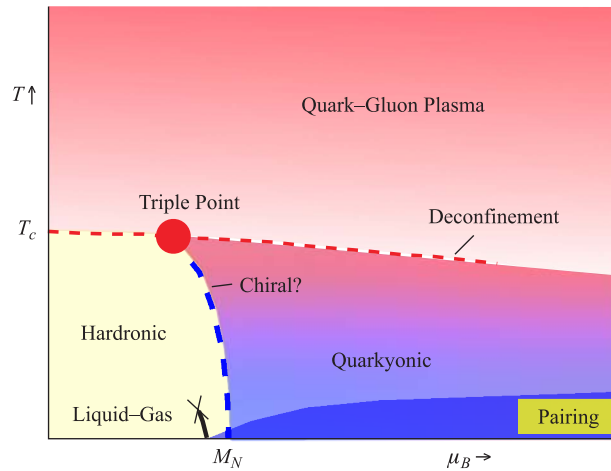


Fig. 7. The revised phase diagram of QCD

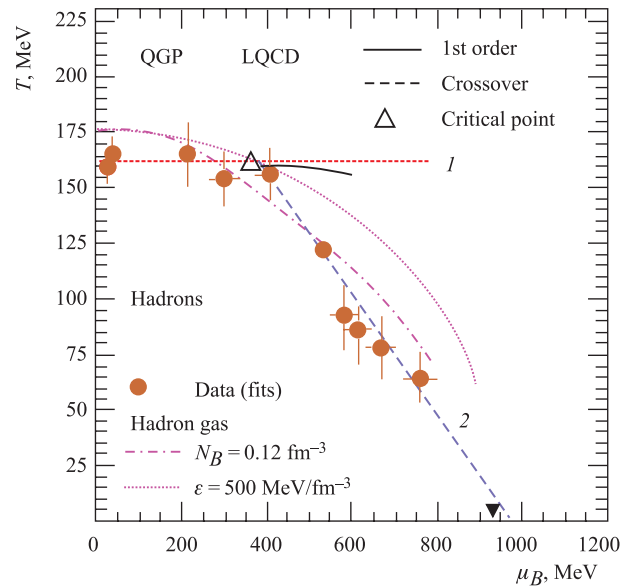


Fig. 8. Chemical potentials and temperatures at decoupling

sition is known to be a crossover. In the FPP–NJL model [14–16], the Hadronic–Quarkyonic transition is first-order [17], but nothing is known from lattice computations. If as we conjecture, there is a region where chiral symmetry is broken by translationally noninvariant modes, then this region must be surrounded by a line of phase transitions. I call this region Happy Island because it is an island of matter in the  $\mu_B - T$  plane.

A remarkable feature of this plot is the triple point where the Hadronic Matter, Deconfined Matter and Quarkyonic Matter all meet [18]. This triple point is reminiscent of the triple point for the liquid, gas and vapor phases of water.

Since we expect a rapid change in the number of degrees of freedom across the transitions among these forms of matter, an expanding system crossing such a transition would undergo much dilution at a fixed value of temperature or baryon chemical potential. One might expect in heavy ions to see decoupling of particle number changing processes at this transition, and the abundances of produced particles will be characteristic of the transition.

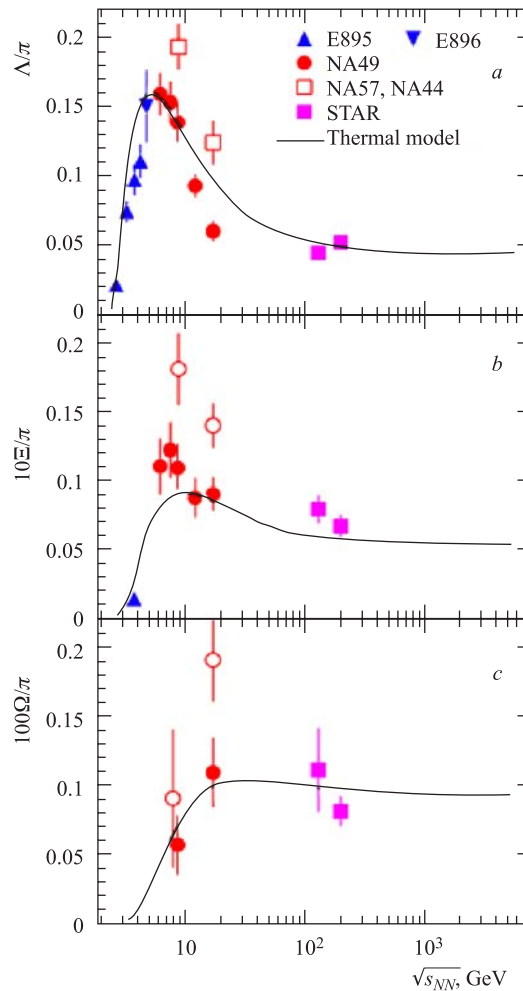


Fig. 9. Ratios of abundances of various particles

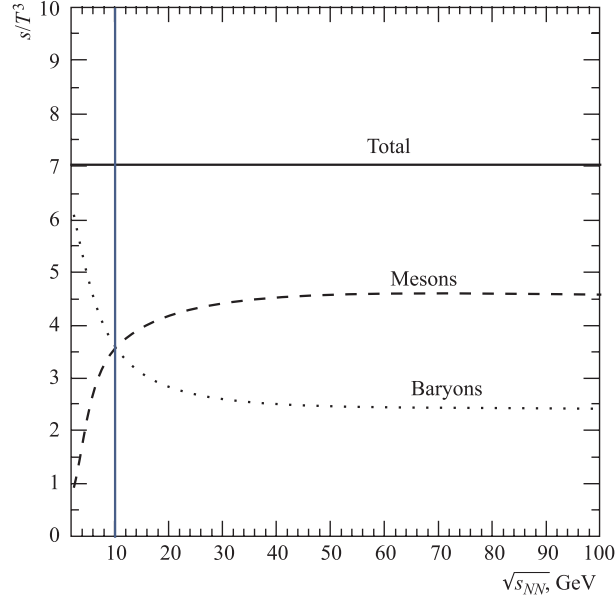


Fig. 10. Energy density stored in baryons compared to that stored in mesons

In Fig. 8, the expectations for the confinement–deconfinement transition are shown with the dotted line 1. It is roughly constant with the baryon chemical potential, and the constant value of temperature is taken from lattice estimates. The dashed curve 2 represents  $\mu_B - T = \text{const} \times M_N$ , corresponding to a simple model for the Quarkyonic transition. Such a very simple description does remarkably well.

A triple point is suggested at a baryon chemical potential near 400 MeV, and temperature near 160 MeV. This corresponds to a center-of-mass energy for Pb–Pb collisions of 9–10 GeV. This is near where there are anomalies in the abundances of ratios of particles [19], as shown in Fig. 9. Shown are fits using statistical models of abundances of particles using chemical potentials and temperature extracted from experimental data. The sharp peak reflects the change in behavior as one proceeds along the dashed line of Fig. 8 corresponding to the Quarkyonic transition and joins to the dotted line 1 of the deconfinement transition.

It is remarkable that the value of beam energy where this occurs corresponds to the hypothetical triple point of Fig. 8, and that this is the density where the energy density stored in baryons becomes equal to that stored in mesons (Fig. 10).

### 3. LECTURE III: THE COLOR GLASS CONDENSATE AND THE GLASMA

The parton distributions of gluons, valence quarks and sea quarks can be measured for some momentum scale less than a resolution scale  $Q$  as a function of their fractional momentum  $x$  of a high energy hadron. The lowest value of  $x$  accessible for a fixed hadron energy  $E$  is typically  $x_{\min} \sim \Lambda_{\text{QCD}}/E_{\text{hadron}}$ . The small  $x$  limit is therefore the high energy limit.

It is remarkable that as  $x$  is decreased, as we go to the high energy limit, the gluon density dominates the constituents of a hadron for  $x \leq 10^{-1}$ . The various distributions are shown as

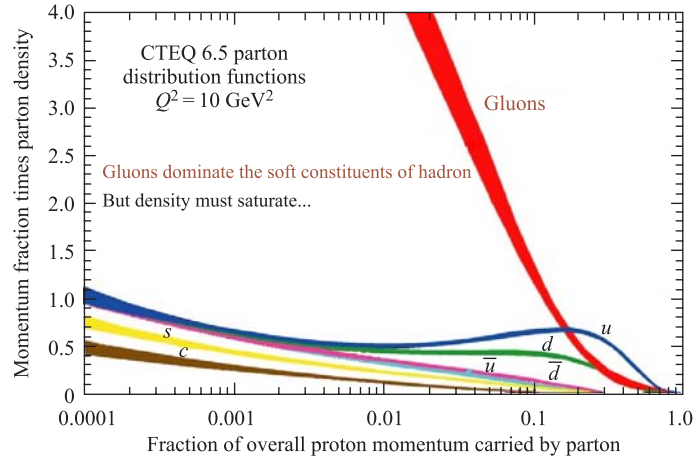


Fig. 11. The parton distribution as a function of  $x$

a function of  $x$  in Fig. 11. The gluon density rises like a power of  $x$  (like  $x^{-\delta}$ ),  $\delta \sim 0.2-0.3$  at accessible energies. The area of a hadron grows slowly with energies. Cross sections grow roughly as  $\ln^2(1/x)$  for small  $x$ . This means that the rapidly growing gluon distribution results in a high density system of gluons. At high density, the gluons have small separation and by asymptotic freedom, the intrinsic strength of their interaction must be weak.

A small intrinsic interaction strength does not mean that interactions are weak. Consider gravity: The interactions between single protons is very weak, but the force of gravity is long range, and the protons in the earth act coherently, that is, always with the same sign. This results in a large force of gravity. This can also happen for the gluons inside a hadron, if their interactions are coherent.

To understand how this might happen, suppose we consider gluons of a fixed size  $r_0 \sim 1/p_T$ , where  $p_T$  is its transverse momentum. We assume that at high energy, the gluons have been Lorentz contracted into a thin sheet, so we need only consider the distribution of gluons in the transverse plane. If we start with a low density of gluons at some energy, and then evolve to higher energy, the density of gluons increases. When the density is of order one gluon per size of the gluon, the interaction remains weak because of asymptotic freedom. When the density is of order  $1/\alpha_S$ , the coherent interactions are strong, and adding another gluon to the system is resisted by a force of order 1. The gluons act as hard spheres. One can add no more gluons to the system of this size. It is however possible to add in smaller gluons, in the space between the closely packed gluons of size  $r_0$ . This is shown in Fig. 12.

The physical picture we derive means that below a certain momentum scale, the saturation scale  $Q_{\text{sat}}$ , the gluon density is saturated and above this scale it is diffuse. The saturation momentum scale grows with energy and need not itself saturate [20–23].

The high phase space density of gluons,  $dN/dy d^2p_T d^2r_T \sim 1/\alpha_S$ , suggests that one can describe the gluons as a classical field. A phase space density has a quantum mechanical interpretation as density of occupation of quantum mechanical states. When the occupation number is large, one is in the classical limit.

One can imagine this high density gluon field generated from higher momentum partons. We introduce the idea of sources corresponding to high  $x$  partons and fields as low  $x$  partons.

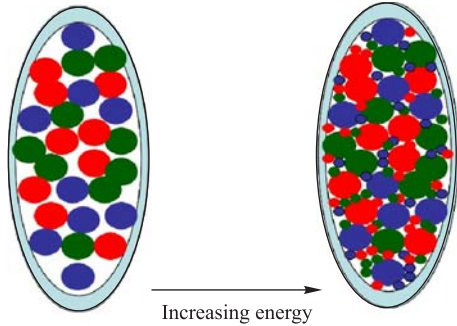


Fig. 12. Increasing the gluon density in a saturated hadron when going to higher energy

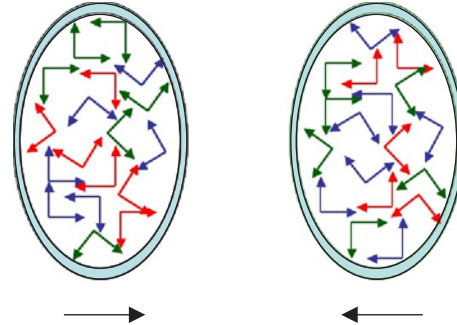


Fig. 13. The collision of two sheets of CGC

Because the high  $x$  parton sources are fast moving, their evolution in time is Lorentz time dilated. The gluon field produced by these sources is therefore static and evolves slowly compared to its natural time scale of evolution. This ultimately means that the different configurations of sources are summed over incoherently, as in a spin glass.

We call this high energy density configuration of colored fields a Color Glass Condensate. The word «color» is used because the gluons that make it are colored. The word «condensate» is used because the phase space density of gluons is large, and because this density is generated spontaneously. The word «glass» is used because the typical time scale of evolution of the classical fields is short compared to the Lorentz time dilated scales associated with the sources of color.

There is an elaborate literature on the Color Glass Condensate and an excellent review is by Iancu and Venugopalan [24]. Evolution of the CGC to small values of  $x$  is understood, as well as many relationships among deep inelastic scattering, deep inelastic diffraction and high-energy nucleus–nucleus, proton–nucleus and proton–proton scattering. The CGC is a universal form of matter in the high energy limit. The theoretical ideas underlying the CGC are largely unchallenged as a description of the high energy limit of QCD, but the issue of when the approximations appropriate for the high energy limit are valid remains contentious.

In the description of high-energy hadron–hadron collisions, we consider the collision of two sheets of CGC as shown in Fig. 13. The color electric and color magnetic fields of the CGC are visualized as sheets of Lenard–Wiechart potentials. These are classical gluon fields whose polarization and color are random, with an intensity distribution determined by the underlying theory of the CGC.

Upon collision of these sheets, the sheets become charged with color magnetic and color electric charge distributions of equal magnitude but opposite sign locally in the transverse plane of the sheets [25–32]. In the high energy limit, sources of color electric and color magnetic field must be treated on an equal footing because of the self-duality of QCD. This induced charge density produces longitudinal color electric and color magnetic fields between the two sheets. These fields are longitudinally boost invariant and therefore have the correct structure to account for Bjorken’s initial conditions in heavy-ion collisions [33]. The typical transverse length scale over which the flux tubes vary is  $1/Q_{\text{sat}}$ . The initial density of

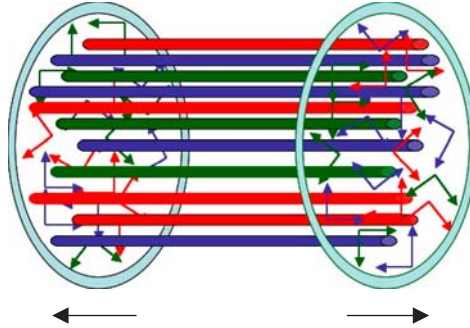


Fig. 14. Glasma flux tube produced after the collision

produced gluons is on dimensional grounds

$$\frac{1}{\pi R^2} \frac{dN}{dy} \sim \frac{Q_{\text{sat}}^2}{\alpha_S}. \quad (16)$$

Because there are both color electric and color magnetic fields, there is a topological charge density of maximal strength induced  $FF^D \sim Q_{\text{sat}}^2/\alpha_S$ .

The decay of products of the Glasma is what presumably makes a thermalized Quark Gluon Plasma. It is not clear how this thermalization takes place. It is quite likely that in the decay of these fields, a turbulent fluid arises, and perhaps this fluid can generate an expansion dynamics similar to that of a thermalized QGP for at least some time [34].

**3.1. Concluding Comments on the CGC and the Glasma.** There is now a wide variety of experimental data largely consistent with the CGC and Glasma-based description. There is a well-developed theoretical framework that provides a robust phenomenology of both electro-hadron scattering and hadron scattering, There will no doubt be future developments related to the LHC. The interested reader is referred to «The Color Glass Condensate: What Have We Learned at RHIC», a workshop held at the RIKEN Brookhaven Center in the winter of 2010.

**Acknowledgements.** I gratefully acknowledge the organizers of the Baikal Summer School on Physics and Astrophysics for putting together this wonderful meeting in a place of such extraordinary beauty. The research of L. McLerran is supported under DOE Contract No. DE-AC02-98CH10886.

#### REFERENCES

1. 't Hooft G. A Planar Diagram Theory for Strong Interactions // Nucl. Phys. B. 1974. V. 72. P. 461.
2. 't Hooft G. A Two-Dimensional Model for Mesons // Ibid. V. 75. P. 461.
3. Witten E. Baryons in the  $1/N$  Expansion // Nucl. Phys. B. 1979. V. 160. P. 57.
4. Thorn C. B. Infinite  $N(C)$  QCD at Finite Temperature: Is There an Ultimate Temperature? // Phys. Lett. B. 1981. V. 99. P. 458.
5. Karsch F. Lattice QCD at High Temperature and Density // Lect. Notes Phys. 2002. V. 583. P. 209; hep-lat/0106019.
6. Bazavov A. *et al.* Equation of State and QCD Transition at Finite Temperature // Phys. Rev. D. 2009. V. 80. P. 014504; hep-lat/0903.4379.

7. *Borsanyi S. et al.* The QCD Equation of State with Dynamical Quarks. hep-lat/1007.2580.
8. *McLerran L., Pisarski R. D.* Phases of Cold, Dense Quarks at Large  $N_c$  // Nucl. Phys. A. 2007. V. 796. P. 83; hep-ph/0706.2191.
9. *Hidaka Y., McLerran L. D., Pisarski R. D.* Baryons and the Phase Diagram for a Large Number of Colors and Flavors // Nucl. Phys. A. 2008. V. 808. P. 117; hep-ph/0803.0279.
10. *Castorina P., Gavai R. V., Satz H.* The QCD Phase Structure at High Baryon Density. arXiv:1003.6078.
11. *Deryagin D. V., Grigoriev D. Y., Rubakov V. A.* Standing Wave Ground State in High Density, Zero Temperature QCD at Large  $N(c)$  // Intern. J. Mod. Phys. A. 1992. V. 7. P. 659.
12. *Kojo T. et al.* Quarkyonic Chiral Spirals. arXiv:0912.3800 (unknown).
13. *Kojo T., Pisarski R., Tsvetik A.* In preparation.
14. *Fukushima K.* Chiral Effective Model with the Polyakov Loop // Phys. Lett. B. 2004. V. 591. P. 277; hep-ph/0310121.
15. *Kaiser N., Fritsch S., Weise W.* Chiral Dynamics and Nuclear Matter // Nucl. Phys. A. 2002. V. 697. P. 255; nucl-th/0105057.
16. *Pisarski R. D.* Quark–Gluon Plasma as a Condensate of  $SU(3)$  Wilson Lines // Phys. Rev. D. 2000. V. 62. P. 111501; hep-ph/0006205.
17. *McLerran L., Redlich K., Sasaki C.* Quarkyonic Matter and Chiral Symmetry Breaking // Nucl. Phys. A. 2009. V. 824. P. 86; hep-ph/0812.3585.
18. *Andronic A. et al.* Hadron Production in Ultrarelativistic Nuclear Collisions: Quarkyonic Matter and a Triple Point in the Phase Diagram of QCD. arXiv:0911.4806 (unknown).
19. *Gazdzicki M., Gorenstein M. I.* On the Early Stage of Nucleus–Nucleus Collisions // Acta Phys. Polon. B. 1999. V. 30. P. 2705; hep-ph/9803462.
20. *Gribov L. V., Levin E. M., Ryskin M. G.* Semihard Processes in QCD // Phys. Rep. 1983. V. 100. P. 1.
21. *Mueller A. H., Qiu J. W.* Gluon Recombination and Shadowing at Small Values of  $x$  // Nucl. Phys. B. 1986. V. 268. P. 427.
22. *McLerran L. D., Venugopalan R.* Computing Quark and Gluon Distribution Functions for Very Large Nuclei // Phys. Rev. D. 1994. V. 49. P. 2233; hep-ph/9309289.
23. *McLerran L. D., Venugopalan R.* Gluon Distribution Functions for Very Large Nuclei at Small Transverse Momentum // Phys. Rev. D. 1994. V. 49. P. 3352; hep-ph/9311205.
24. *Iancu E., Venugopalan R.* The Color Glass Condensate and High Energy Scattering in QCD. hep-ph/0303204.
25. *Kovner A., McLerran L. D., Weigert H.* Gluon Production from Non-Abelian Weizsacker–Williams Fields in Nucleus–Nucleus Collisions // Phys. Rev. D. 1995. V. 52. P. 6231; hep-ph/9502289.
26. *Kovner A., McLerran L. D., Weigert H.* Gluon Production at High Transverse Momentum in the McLerran–Venugopalan Model of Nuclear Structure Functions // Phys. Rev. D. 1995. V. 52. P. 3809; hep-ph/9505320.
27. *Krasnitz A., Venugopalan R.* Nonperturbative Computation of Gluon Mini-Jet Production in Nuclear Collisions at Very High Energies // Nucl. Phys. B. 1999. V. 557. P. 237; hep-ph/9809433.
28. *Krasnitz A., Venugopalan R.* The Initial Energy Density of Gluons Produced in Very High Energy Nuclear Collisions // Phys. Rev. Lett. 2000. V. 84. P. 4309; hep-ph/9909203.
29. *Krasnitz A., Venugopalan R.* The Initial Gluon Multiplicity in Heavy Ion Collisions // Phys. Rev. Lett. 2001. V. 86. P. 1717; hep-ph/0007108.
30. *Krasnitz A., Nara Y., Venugopalan R.* Coherent Gluon Production in Very High Energy Heavy Ion Collisions // Phys. Rev. Lett. 2001. V. 87. P. 192302.

31. *Lappi T.* Production of Gluons in the Classical Field Model for Heavy Ion Collisions // *Phys. Rev. C.* 2003. V. 67. P. 054903; hep-ph/0303076.
32. *Lappi T., McLerran L.* Some Features of the Glasma // *Nucl. Phys. A.* 2006. V. 772. P. 200; hep-ph/0602189.
33. *Bjorken J. D.* Highly Relativistic Nucleus–Nucleus Collisions: The Central Rapidity Region // *Phys. Rev. D.* 1983. V. 27. P. 140.
34. *Dusling K. et al.* Role of Quantum Fluctuations in a System with Strong Fields: Onset of Hydrodynamical Flow. hep-ph/1009.4363.